Stress and large-scale spatial structures in dense, driven granular flows

Allison Ferguson and Bulbul Chakraborty
Martin Fisher School of Physics, Brandeis University, Mailstop 057, Waltham, Massachusetts 02454-9110, USA
(Received 16 June 2005; published 12 January 2006)

We study the appearance of large-scale dynamical heterogeneities in a simplified model of a driven, dissipative granular system. Simulations of steady-state gravity-driven flows of inelastically colliding hard disks show the formation of large-scale linear structures of particles with a high collision frequency. These chains can be shown to carry much of the collisional stress in the system due to a dynamical correlation that develops between the momentum transfer and time between collisions in these frequently colliding particles. The lifetime of these dynamical stress heterogeneities is seen to grow as the flow velocity decreases toward jamming, leading to slowly decaying stress correlations reminiscent of the slow dynamics observed in supercooled liquids.

DOI: 10.1103/PhysRevE.73.011303 PACS number(s): 81.05.Rm, 45.70.−n, 83.10.Pp

I. INTRODUCTION

Granular materials are ubiquitous in nature and play an important role in many industrial applications, yet the appropriate coarse-grained theories for the description of these materials remain elusive due to the rich phenomenology they display in response to external perturbation [1,2]. A common example of the unusual nature of granular systems is the phenomenon of force chains, highly stressed extended linear clusters first seen in experiments on static granular piles [3]. These striking inhomogeneities are thought to be responsible for a host of observed nonlinear effects in static systems including interesting features in distributions of contact forces between particles [4]. However, the reason for the existence of the force chains has not been determined; one possible explanation is that correlations develop while the material is flowing which then get "frozen in" when the system comes to rest.

Spatial structures have been directly observed in experiments on flowing granular materials [5]. More recently, measurements of velocity correlations in the surface layer of particles flowing down an inclined plane have yielded a length scale which appears to grow as the flow is arrested [6]. While detection of such dynamical heterogeneities in numerical studies has been more difficult, there is some evidence for their existence in simulations of gravity-driven flow through a hopper [7] and in images of the contact force network in simulations of chute flow [8]. The presence of such structures will play a crucial role in determining the dynamics of the flowing system, especially as the transition to a static system is approached. The development of spatial and temporal correlations near the transition to the static state must be investigated carefully in order to understand the nature of the transition from the flowing liquid state.

Dynamical heterogeneities have been observed in other systems which exhibit a similar slow dynamics as the transition from fluid to solid is approached, such as colloids near the glass transition. Fast-moving particles were observed to be spatially correlated with a characteristic cluster size that increased as the glass transition was approached [9]. In supercooled liquids, spatial inhomogeneities can be identified via a time-dependent four-point (two-time, two-space) correlation function [10]. The interesting commonalities between these disparate systems have been explored in the context of the jamming phase diagram proposed in Refs. [11,12]. It should be noted that in these studies the focus has been primarily on the search for a common static signature [i.e., the distribution of contact forces $P(f)$]. Thus the proper framework to describe the dynamics of systems that have a jamming transition remains an open question. If the presence of dynamical heterogeneities governs the dynamics of these far-from-equilibrium systems near the jamming transition, then while the microscopic process by which these structures form may vary between different types of systems, some unified dynamical description may be applicable once the structures have formed. The "soft glassy rheology" model [13,14] describes soft, nonergodic systems such as foams and dense emulsions and has successfully predicted many of the experimentally observed results. Application of this type of "traplike dynamics" to granular systems has also had some promising initial results [15].

In this paper we explore the connections between dynamical heterogeneities and slow dynamics in a simplified model which allows us to focus on the essential effects of driving and dissipation in a flowing granular system, while still reproducing observable results from related experimental systems [16]. Simulations have been performed of a two-dimensional gravity-driven system of frictionless, bidisperse hard disks in a hopper geometry. The disks undergo instantaneous, inelastic binary collisions and propagate under gravity in between collision events. Despite the simplified dynamics of the simulation, several interesting collective effects are seen to emerge. As in previous studies [7], extended linear structures defined by inhomogeneities in the spatial distribution of the collision frequency are visible, and their presence has a measurable effect on distributions of impulse and time intervals between collisions for a given particle. In this study we observe that the particles which make up the linear structures display a dynamic correlation between their impulse and collision time which is reflected in measurements of the collisional stress tensor; particles identified as part of the structures appear to experience higher than average collisional stress compared with the remainder

of the system. Using this measure of collisional stress we can probe further into the nature of these structures and their relevance to the dynamics of the system.

II. SIMULATIONS

The grain dynamics used in the simulations are similar to those in Ref. [17]. Specifically, (i) at each interparticle collision, momentum is conserved but the collisions are inelastic so the relative normal velocity is reduced by the coefficient of restitution μ; (ii) to allow the side walls to absorb some vertical momentum we impose the condition that collisions with the walls are inelastic with a coefficient of restitution μ_{wall} in the direction tangential to the wall; and (iii) since we wish to observe the system over many events, particles exiting the system at the bottom must be replaced at the top to create uniform, sustained flow. Note that collisions are instantaneous and in between collisions the particles are driven by gravity. To avoid the phenomenon of inelastic collapse the coefficients of restitution μ and μ_{wall} are velocity dependent; if the relative normal velocity between particles or between a given particle and the wall is less than some cutoff v_{cut} then the collision is presumed to be elastic [18]. The flow velocity v_f is controlled by adjusting the width of the hopper opening. We also introduce a probability of reflection p at the bottom which reduces the time needed to reach steady-state flow. Typically, our simulations were done on bidisperse systems (diameter ratio 1:1.2) of 1000 disks, with $\mu=0.8$, $\mu_{wall}=0.5$, $v_{cut}=1\times10^{-3}$, and $p=0.5$. The simulation was run for a total time of 1×10^3 in simulation time units (smaller particle diameter d_s and gravitational constant g are both set to 1) with the initial time interval of 5×10^2 discarded before recording data to ensure the system has reached steady state. During the total time interval of 500 over which we are evaluating the data, a given particle will pass through the hopper 5–10 times depending on the flow velocity.

As the width of the hopper opening is decreased the average flow velocity decreases, and at some minimum opening sustained flow is no longer observed. Close to this width the mass flow exiting the hopper appears to become very intermittent, with large outflow of mass occurring on short time scales followed by long time intervals where few particles exit the system. Intermittent dynamics has also been observed in simulations of flow down an inclined plane where the angle of incline is approximately equal to the angle of repose of the grains [8]. Additionally, some preliminary measurements of spatial velocity correlations in our hopper simulations parallel to the flow direction indicate long range correlations on length scales comparable to the system size for slow flow velocities [19]. Spatial velocity correlations with long length scales are also seen on the surface of incline plane flow [6].

III. COLLISION FREQUENCY AND LARGE-SCALE STRUCTURES

In studies of two dimensional freely cooling gases [20] some evidence of dynamical large-scale structures forming in the system was first observed by identifying all particles

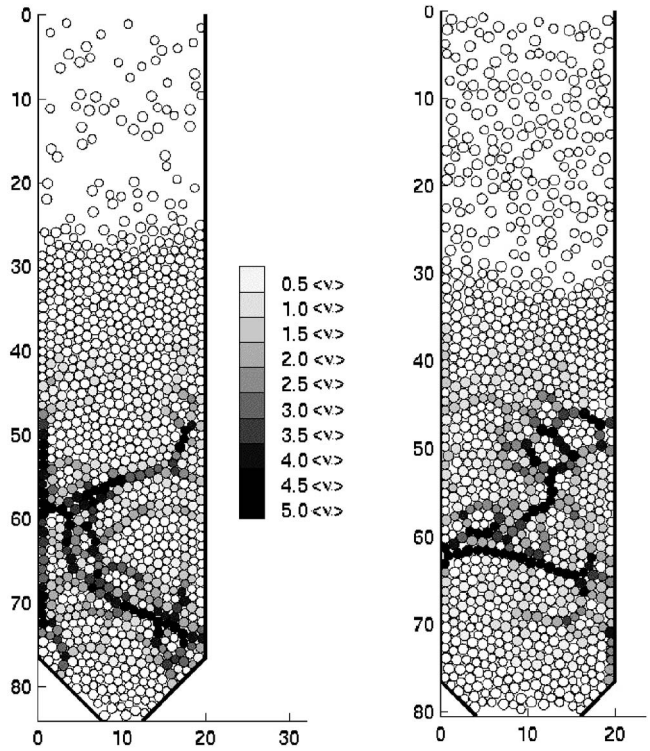

FIG. 1. Images of the system with particles colored according to the collision frequency in the last time interval $\Delta t=0.02$ for $v_f=0.86$ (left) and $v_f=2.2$ (right). $\langle\nu\rangle$ is defined as the mean collision frequency (average taken over all particles) for that time interval.

experiencing inelastic collapse as the assembly of grains cooled. These particles formed linear structures within dense clusters and experienced collision frequencies significantly higher than that of the other particles in the system. Due to the effect of driving in our flowing system, we do not observe inelastic collapse. However, we can ask an analogous question: "How many collisions does a given grain undergo in a given time interval Δt?" The collision frequency for a particular particle i in Δt is given by $\nu_i=N_i/\Delta t$ where N_i is the number of collisions experienced by particle i in Δt. We can construct images of our simulated system at regular intervals and color individual disks according to the value of the collision frequency for that disk. As can be seen in Fig. 1 particles with high collision frequencies form linear chains reminiscent of the structures observed in two-dimensional (2D) freely cooling gases and the transient solid chains postulated by the hydrodynamic model of Ref. [21]. These chains often appear to terminate at the boundary of the system, forming an archlike structure in the center of the hopper. From the pictures it is also evident that collision direction is typically oriented along the chain direction (i.e., particles within a chain collide with other particles in the chain and not with neighboring particles that are not part of the structure). Thus the velocities of frequently colliding particles are highly correlated in direction, and we can evaluate the stability of this structure with respect to perturbations arising from collisions with other (uncorrelated) particles. Consider an initially isotropically distributed dense assembly

of completely correlated disks and perturb one disk by giving it a velocity $\mathbf{v}$. The collision rule for two inelastic hard disks i,j is [17]

$$\begin{bmatrix} \mathbf{v}_i' \\ \mathbf{v}_j' \end{bmatrix} = \begin{bmatrix} \mathbf{v}_i \\ \mathbf{v}_j \end{bmatrix} + \frac{1+\mu}{2}\begin{bmatrix} -\mathbf{v}_i\cdot\mathbf{q}+\mathbf{v}_j\cdot\mathbf{q} \\ \mathbf{v}_i\cdot\mathbf{q}-\mathbf{v}_j\cdot\mathbf{q} \end{bmatrix}\mathbf{q} \tag{1}$$

where $\mathbf{q}$ is a unit vector along the center of mass line of the colliding disks and $\mathbf{v}'$ denotes the velocity of a given particle after the collision. Rewriting Eq. (1) in terms of the relative velocity of particle j to particle i before the collision $\delta\mathbf{v}(t)=\mathbf{v}_j-\mathbf{v}_i$ and after the collision $\delta\mathbf{v}(t+\Delta t)=\mathbf{v}_j'-\mathbf{v}_i'$, we can obtain an approximate expression for the time derivative of the relative velocity in the limit of $\Delta t\to 0$:

$$\frac{d\delta\mathbf{v}(t)}{dt} \simeq \frac{1+\mu}{\Delta t}[-\delta\mathbf{v}(t)\cdot\mathbf{q}]\mathbf{q}. \tag{2}$$

Define $q_\parallel$ and $q_\perp$ as the components of $\mathbf{q}$ parallel and perpendicular, respectively, to the initial perturbing velocity. From Eq. (2) it is easy to see that $\langle d\delta v_\parallel/dt\rangle \simeq -C_q\langle q_\parallel\rangle$ and $\langle d\delta v_\perp/dt\rangle \simeq -C_q\langle q_\perp\rangle$, where $C_q=[(1+\mu)/\Delta t]\langle\delta v(t)\cos(\theta_{vq})\rangle$ (θ_{vq} is the angle between $\delta\mathbf{v}$ and $\mathbf{q}$) and the angular brackets denote an average over collisions. The factor C_q can be taken outside of the angular brackets when performing the average of Eq. (2) as the initial relative velocity vector $\delta\mathbf{v}$ is uncorrelated in direction with the center of mass line vector $\mathbf{q}$.

However, $q_\perp$ is equally likely to be positive or negative so that $\langle q_\perp\rangle\sim 0$ while $q_\parallel$ is always positive and so $\langle q_\parallel\rangle>0$. Substituting this result into the above expressions for the time derivatives yields $\langle d\delta v_\parallel/dt\rangle<0$ and $\langle d\delta v_\perp/dt\rangle\sim 0$ indicating that velocity differences parallel to the initial perturbation will decay while velocity differences perpendicular to $\mathbf{v}$ will remain. Given this, and the organizing influence of the inelastic wall collisions leading to velocities becoming normal to the wall, the appearance of collisional chains anchored to the wall becomes plausible.

IV. STRESS

The unusual rheology of granular matter in response to external stress as well as the phenomena of force chains prompt us to investigate stress in this simple model of flowing granular matter. Specifically, are the frequently colliding chains described in the previous section the dynamical analog of force chains? We can explore this possible connection by measuring the stress in our system and determining if a correspondence exists between the collisional chains and the spatial distribution of stress. Additionally, we can potentially use the measured stress to calculate relevant time and length scales associated with the structures, as well as making a clearer connection between our model and other systems with soft, glassy rheology.

As described in Ref. [22], macroscopic stress in discrete particle systems develops as a result of two microscopic mechanisms of momentum transfer: (a) transport of momentum due to the fluctuations of the individual particle velocities (the kinetic stress σ_k) and (b) transport of momentum at interparticle collisions (the collisional stress σ_c). The total stress tensor is then the sum of the kinetic and collisional stresses. However, for the densities we observe, we find as in Ref. [22] that the magnitude of the kinetic stress contribution is several orders of magnitude lower than the collisional stress. Thus we will consider only the collisional stress contribution in the analysis to follow. For a given particle i, the $\mu\nu$ component of the collisional part of the stress tensor at time t is given by

$$\sigma_{c,i}^{\mu\nu}(t) = \frac{1}{\Delta t}\sum_\alpha (\mathbf{I}_\alpha\cdot\mathbf{r}_{i\alpha})\hat{r}_{i\alpha}^\mu\hat{r}_{i\alpha}^\nu \tag{3}$$

where μ,ν are Cartesian coordinates and $\mathbf{I}_\alpha$ is the impulse transferred to particle i at collision α. The sum is taken over all of the collisions experienced by particle i during time $t-\Delta t\to t$, where the interval Δt is chosen such that $\langle\tau\rangle\ll\Delta t\ll 1/v_f$ where τ is the time between successive collisions for a particular particle. This constraint ensures that the particle being evaluated experiences many collisions during Δt but is not significantly rearranging relative to its neighbors. There is a separation of time scales (which will be demonstrated more concretely in the analysis to follow) that ensures an interval Δt satisfying this constraint is easy to locate. Note that for hard-disk collisions $\mathbf{I}_\alpha$ will always be along $\mathbf{r}_{i\alpha}$; therefore the $\mathbf{I}_\alpha\cdot\mathbf{r}_{i\alpha}$ term in the sum is simply $(d_i+d_j)I_\alpha/2$ where d_i and d_j are the diameters of particle i and the other particle involved in collision α, respectively.

Similarly to the images of the system at a given time t constructed for the collision frequency, we can make complementary images of $\sigma_c(t)$ (Fig. 2). For every particle we calculate $\sigma_c(t)$ as described in Eq. (3), and extract the maximum eigenvalue λ_m along with the corresponding principal axis. A line along the direction of this principal axis is plotted at the particle position, and then colored according to the value of λ_m relative to the average value of the maximum eigenvalue measured in that time interval $\langle\lambda\rangle$. Figure 2 shows some sample images constructed in this way for the same systems and times as in Fig. 1. Comparison of the two figures reveals a strong correlation between the frequently colliding particles and the highly stressed particles. Additionally, the principal axis of the stress for the highly stressed and frequently colliding particles is typically aligned along the chain direction. There is also a lack of an obviously growing length scale as $v_f\to 0$; however, time scales associated with these highly stressed structures show a significant change with flow velocity as discussed below.

Note that the value of λ_m will depend on the ratio $\Sigma_\alpha I_\alpha/\Delta t$, and thus, since the frequently colliding particles experience many collisions in Δt (i.e., $\nu_i\propto 1/\tau\gg\langle\nu\rangle$, where τ is the time between successive collisions for a particular particle), then the sum over I_α can be large even if the average impulse per collision is small. Thus λ_m [and similarly $\sigma_c(t)$] will depend crucially on the ratio of impulse I and collision time τ, and any correlation between these quantities. Therefore, to gain a better understanding of the correspondence between the frequently colliding particles and the highly stressed particles we have studied the joint distribution of impulse and collision time $P(I,\tau)$.

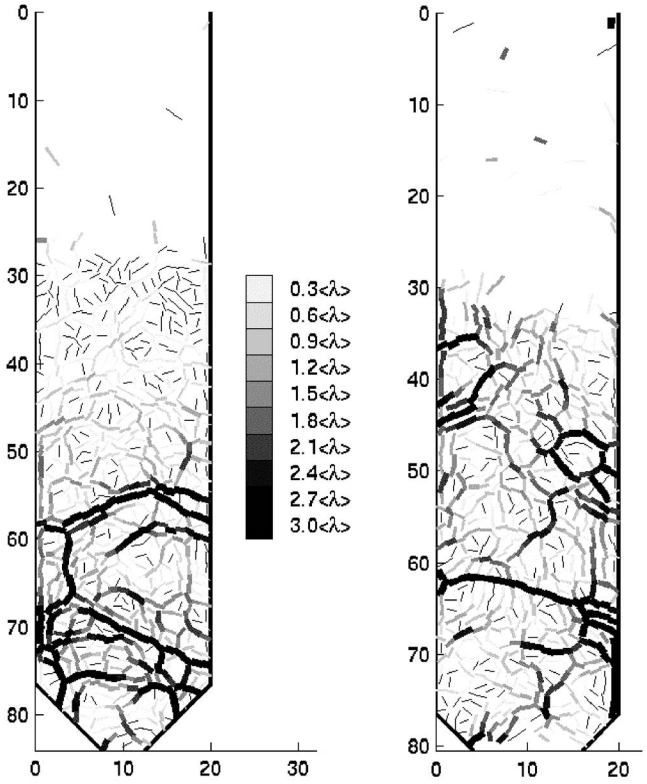

FIG. 2. Images of the system with principal axis corresponding to the maximum eigenvalue λ_m of the collisional stress tensor defined during the last time interval $\Delta t=0.02$ for $v_f=0.86$ (left) and $v_f=2.2$ (right) plotted at the particle positions. The principal axis line is colored and its width scaled according to the magnitude of the maximum eigenvalue λ_m (the thicker the line the higher the value of λ_m). Thin black lines indicate the principal axis of particles experiencing less than the minimum stress plotted ($0.3\langle\lambda\rangle$ for these pictures). Note that these pictures were constructed for the same time interval as the images in Fig. 1. $\langle\lambda\rangle$ is defined as the mean λ_m (average taken over all particles) for that time interval.

V. DISTRIBUTIONS OF IMPULSE AND COLLISION TIME

In previous work [7] we modeled recent experiments on dense, gravity-driven monodisperse granular flows [16]. These experiments consisted of a quasi-2D system of monodisperse steel spheres flowing through a hopper. A transducer (of size approximately equal to the diameter of the spheres) was placed a short distance upstream from the opening at the bottom of the hopper, allowing for measurements of impulse normal to the hopper wall as a function of time. Both the experiments of Ref. [16] and the simulations we performed measured the distribution of impulses transferred at each collision, $P(I)$, as well as the distribution of time intervals between the instantaneous collisions, $P(\tau)$. In the experiment the measurement was made at the wall by using a transducer positioned a short distance upstream from the hopper opening to detect the impulse transfer as a function of time to that point on the wall. In the simulation we can separately analyze data from events located within the bulk, at the walls, or at a specific point on the wall to mimic the experimental measurement. For most of our discussion we will focus on observations of distributions taken from events occurring in the bulk of the material. Note that all our measurements were made in the central, vertical region of the hopper ($5<x<15$, $35<y<65$) where the slow velocity averaged over a (snapshot) time had no significant spatial variation.

Both the experiment and the simulation revealed the same effects in the measured distributions: (i) an increase in the number of small-impulse events as the flow velocity is decreased as well as (ii) an increase in the number of small-collision-time events as the flow velocity is decreased. In the impulse distribution in particular, this change could be directly linked to the appearance of the frequently colliding clusters pictured above. Additionally, a simple one-dimensional model was devised that demonstrated how the existence of linear clusters of particles which collide primarily along the chain direction would lead to the observed behavior in $P(I)$ [7]. The flow-rate invariant exponential form of $P(I)$ at large impulse as measured in both experiment and simulation was shown to be a reflection of the local velocity distribution, which had an exponential tail (note that the impulse distribution of uncorrelated particles is essentially the convolution of the individual velocity distributions). Using the same 1D toy model we were able to demonstrate that the large-impulse region of $P(I)$ is determined primarily by the form of the velocity distribution as observed.

In the bidisperse system, the picture retains many of its original features with some added complexity. Defining the scaled impulse $\tilde{I}=I/\langle I\rangle$ where $\langle I\rangle=\int IP(I)dI$ we can consider the behavior of the joint distribution of impulse and collision time $P(\tilde{I},\tau)$. Shown in Fig. 3(a) as a function of $\tilde{I}$ for two values of τ, several interesting features are seen to emerge. For both values of τ, $P(\tilde{I},\tau)$ still shows an increase in height at impulses smaller than the average impulse as the flow velocity is decreased. However, for $\tau=10^{-3}$ the large-impulse region of the distribution is no longer flow-rate independent as in the monodisperse system, and an increase in height at impulses much larger than the average is also visible [23]. As before, this large-impulse behavior can be linked to an accompanying shape change in the velocity distribution [Fig. 3(b)], and is similar to the behavior of $P(\tilde{I})$ in three-dimensional molecular dynamics simulations of soft spheres [24]. The shape of the collision time distribution $P(\tau)$ is very broad, and approaches $\tau^{-5/2}$ as the flow velocity is slowed. The nonexponential nature of $P(\tau)$ implies that the interparticle collisions are correlated to some extent. These correlations are also reflected in the anomalous diffusivities measured in experiments on granular drainage [25].

If we look at $P(\tilde{I},\tau)$ as a function of $\tilde{I}$ for a given flow velocity, it is evident that the impulse and collision time are correlated (i.e., small impulses tend to be associated with small collision times). To clarify the roles played by the frequently colliding and rarely colliding particles in the observed shape changes in $P(\tilde{I},\tau)$ we can divide the joint impulse–collision time distribution into contributions from these two populations (shown in Fig. 4 for $v_f=1.13$). For this purpose, based on review of the images we chose a threshold frequency of $5\langle\nu\rangle$ where $\langle\nu\rangle=(1/N)\Sigma_i^N\nu_i$ and defined all par-

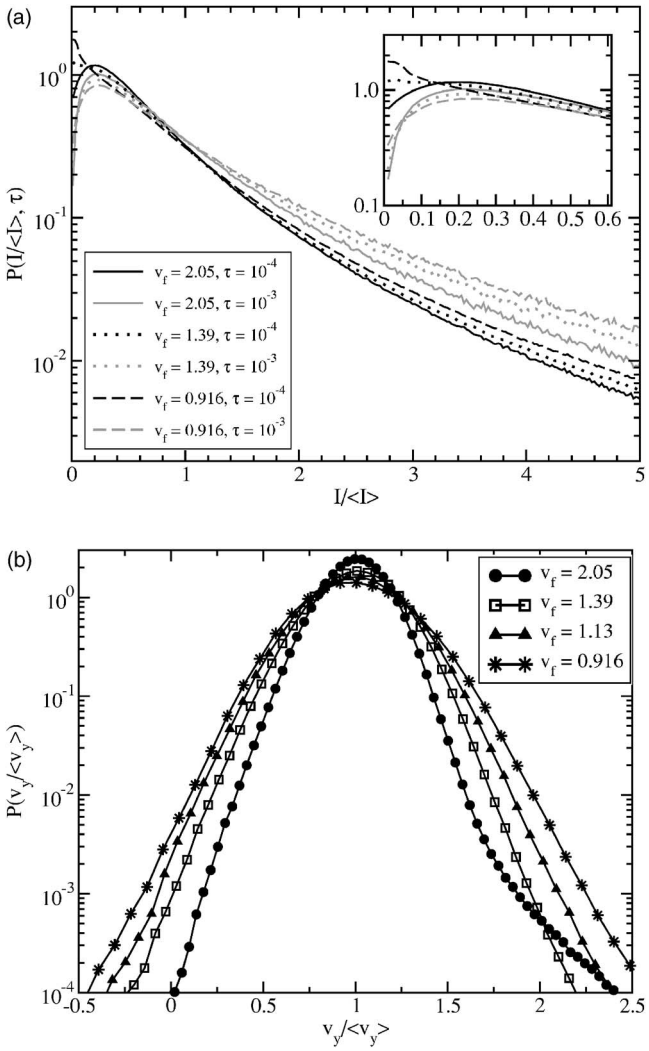

FIG. 3. (a) Joint impulse–collision time distribution $P(\tilde{I},\tau)$ at varying flow velocities. The inset shows the small-impulse region of the distribution in more detail. Note that the two cuts of $P(\tilde{I},\tau)$ have been separately normalized for easier comparison. (b) Corresponding velocity distributions $P(v_y/\langle v_y\rangle)$.

ticles with collision frequency ν_i above this threshold as frequently colliding. Rarely colliding particles are similarly defined as particles with $0<\nu_i<0.5\langle\nu\rangle$. It appears that the correlation between impulse and collision time is stronger for the frequently colliding particles, and that these particles are the primary contributors to $P(\tilde{I},\tau)$ at small $\tilde{I}$ and τ [26]. Additionally, as expected from the observations made on the large-impulse region of the total $P(\tilde{I},\tau)$, at longer collision times and large impulses the shape of the distribution is governed by the contribution from the rarely colliding particles [which in turn reflects the shape changes in the velocity distribution shown in Fig. 3(b)].

The impulse–collision time correlation observed in $P(\tilde{I},\tau)$ is further evidence that velocities of frequently colliding particles are correlated with small fluctuations leading to collisions with $\tilde{I}<1$. Note that this correlation in the velocities is apparent even in the absence of any density inhomogeneity.

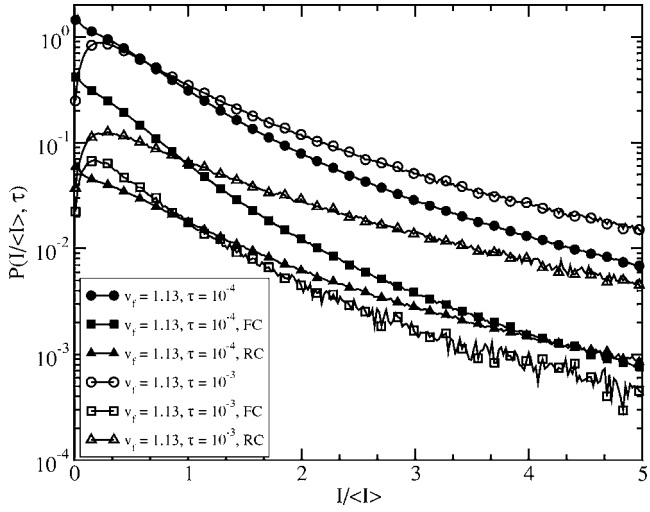

FIG. 4. Impulse distribution $P(\tilde{I},\tau)$ showing the separate contribution from the frequently colliding (FC) particles ($\nu_i>5\langle\nu\rangle$) and the rarely colliding (RC) particles ($\nu_i<0.5\langle\nu\rangle$) at $v_f=1.13$.

The connection between the frequently colliding particles and the highly stressed particles is not surprising in the context of the impulse–collision time correlation discussed above, which would give rise to values of $\lambda_m \gg \langle\lambda\rangle$. Therefore the stress heterogeneities seen in Fig. 2 are directly related to the dynamic correlation reflected in $P(\tilde{I},\tau)$. Given that this correlation is seen to become stronger as the flow velocity decreases, it is reasonable to expect some kind of flow-rate dependent behavior in time and length scales associated with the collisional stress. As previously described, there does not appear to be any significant change in length scale of the structures with flow velocity. As a first attempt to quantify a trend in the time scale, we will calculate the autocorrelation $C_\lambda(t)$ of λ_m and determine the dependence of the time scale for the decay of $C_\lambda(t)$ on v_f.

VI. RELAXATION OF STRESS

The autocorrelation of the maximum eigenvalue $C_\lambda(t)=\langle\lambda_m(t)\lambda_m(0)\rangle$ of λ_m is calculated as

$$\langle\lambda_m(t)\lambda_m(0)\rangle = \frac{1}{NN_{t_0}}\sum_{i,t_0}(\lambda_m(t_0)-\langle\lambda_m\rangle)(\lambda_m(t_0+t)-\langle\lambda_m\rangle) \tag{4}$$

where $\langle\lambda_m\rangle$ is the time-averaged value of the maximum eigenvalue and N_{t_0} is the number of time origins t_0. $C_\lambda(t)$ (shown in Fig. 5 for varying flow velocities) appears to have three decay regimes: (i) a short power-law regime at small time $t\sim\langle\tau\rangle$, (ii) a longer slow (possibly logarithmic) decay at intermediate time $\langle\tau\rangle\ll t\ll 1/v_f$, and (iii) a more complicated decay at long time $t\gg 1/v_f$ which involves a shallow negative dip. This three-stage form of $C_\lambda(t)$ is reminiscent of density-density autocorrelations measured in supercooled liquids at low temperatures [27], which show a power-law regime at short time scales, a plateau at intermediate time

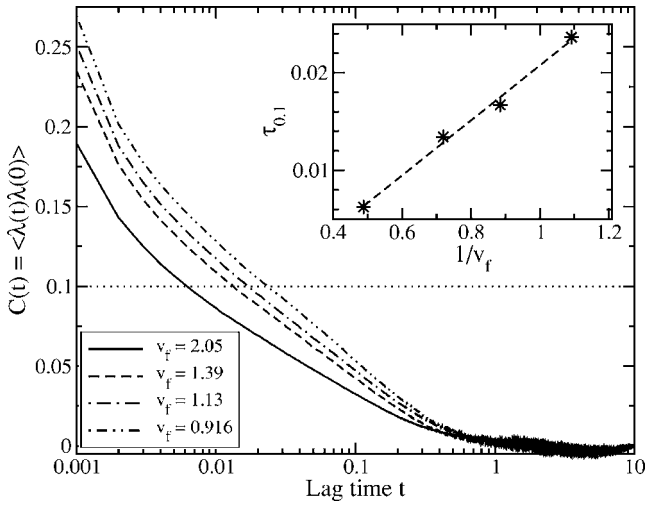

FIG. 5. Autocorrelation of maximum eigenvalue λ_m of $\sigma_c(t)$. Inset shows the time scale $\tau_{0.1}$ at which $\langle\lambda_m(t)\lambda_m(0)\rangle=0.1$ plotted against $1/v_f$.

scales, and a decay to zero at much longer time scales. This implies that the intermediate slow decay observed in the granular system may be resulting from a type of "caging effect" introduced by the correlated motion of particles participating in one of the highly stressed and frequently colliding chains. This type of $C_\lambda(t)$ indicates a growing separation of time scales as the flow velocity is decreased, which is an interesting similarity between granular flows and supercooled liquids.

We can get a measure of the time scale associated with this intermediate slow decay of the stress by extracting the time $\tau_{0.1}$ at which $C_\lambda(t)$ has decayed to 10% of its original value (i.e $C_\lambda(\tau_{0.1})=0.1$). Plotting $\tau_{0.1}$ vs $1/v_f$ (see inset to Fig. 5) clearly indicates that $\tau_{0.1}$ diverges as $1/v_f$. If we associate this time scale with the lifetime of the highly stressed spatial structures visible in Fig. 2 then one can see that as the flow velocity decreases the structures last for increasingly longer times. $C_\lambda(t)$ for the frequently colliding particles only is shown in Fig. 6(a). These curves were calculated by choosing only those time origins t_0 where a given particle had been identified as frequently colliding according to the criteria defined above ($\nu_i > 5\langle\nu\rangle$). Note the particle is not required to be frequently colliding during the entire time interval over which $C_\lambda(t)$ is calculated, thus we expect the long time behavior of these curves to be similar to that of the entire system. The same three-regime behavior is evident, but the time scale of the decay $\tau_{0.1}^{FC}$ is longer ($\tau_{0.1}^{FC}=2\tau_{0.1}$). However, the scaling of the decay time with the flow velocity is the same [see inset to Fig. 6(a)].

The role of the frequently colliding and highly stressed particles in determining the shape of the autocorrelation can be clarified by considering a related system; a one-dimensional assembly of particles which experience instantaneous, binary, inelastic collisions. To establish a steady state, a fraction of the particles are weakly driven in between collision events. This 1D system represents an idealized, isolated analog to the frequent-collision chains, and thus the stress autocorrelation measured in this system should be representative of the stress relaxation behavior of these structures [note that $\sigma_c(t)$ in the 1D system is a scalar quantity]. $C_\lambda(t)$ for the 1D system is shown in Fig. 6(b) [28]. From this plot it can be seen that the initial stress relaxation is slow and possibly logarithmic, similar to the slow decay regime of $C_\lambda(t)$ in the 2D flowing system. From this result it appears that the observed dynamical heterogeneities do dominate the stress relaxation in the flowing granular system at intermediate time scales $\langle\tau\rangle \ll t \ll 1/v_f$.

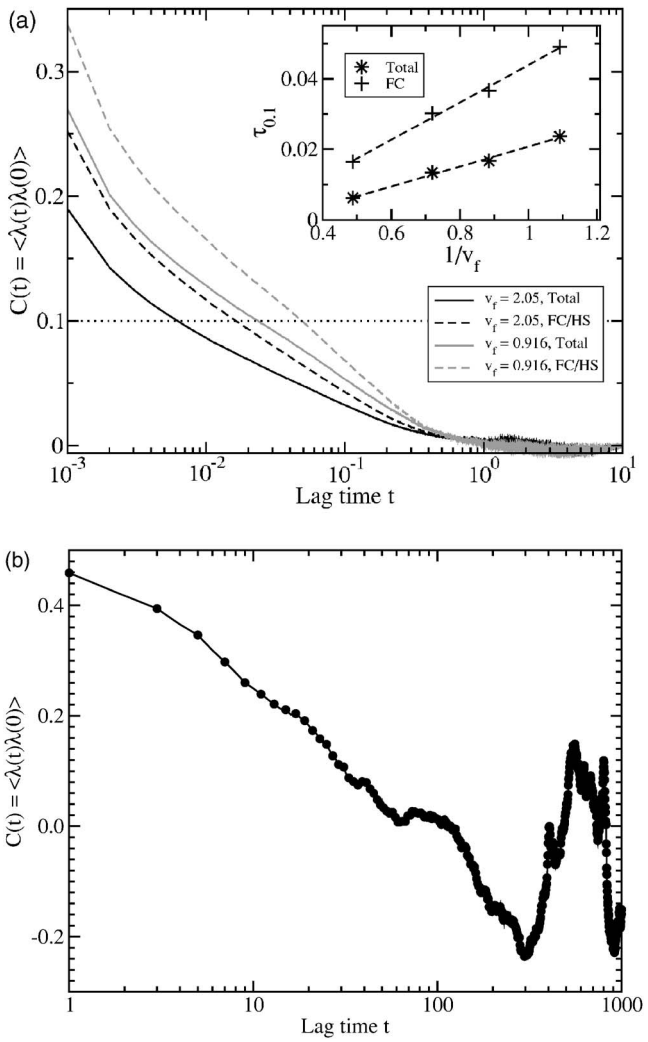

FIG. 6. (a) Autocorrelation of maximum eigenvalue λ_m of $\sigma_c(t)$ for both the frequently colliding (FC) particles and the whole system at $v_f=2.05$ and $v_f=0.916$. Inset shows the time scale $\tau_{0.1}$ at which $\langle\lambda_m(t)\lambda_m(0)\rangle=0.1$ plotted against $1/v_f$ for both the FC particles and the whole system. (b) Stress autocorrelation for 1D weakly driven inelastic granular gas.

VII. CONCLUSIONS

The picture which is emerging from these simulations is that large-scale highly stressed structures analogous to force chains in static systems can form even in a simplified model of inelastic hard disks. These structures experience a slow relaxation from collisional stress at intermediate time scales in a manner analogous to temporal relaxations observed in glassy systems at low temperatures. Additionally, the time

scale extracted from measurements of the stress relaxation curve $C_\lambda(t)$ is seen to diverge as $1/v_f$. This time scale can be associated with the average lifetime of a highly stressed and/or frequently colliding chain in the system and thus the chains appear to become infinitely long lived as $v_f \to 0$.

It is worth noting that a similar search for a relevant length scale associated with these chains has been more difficult. Simple two-point spatial correlations of the collisional stress have not yielded any meaningful results and thus a higher-order correlation function such as the four-point correlations measured in supercooled liquids [10] measured may be necessary. Initial calculations of spatial velocity correlations in our flowing system have indicated the existence of a length scale which is increasing as the flow velocity is decreased [19]. Preliminary measurements show that this length scale is of the order of the system size at the slowest flow velocities measured thus far. Therefore another important consideration is finite-size effects; while we have not explored this issue in this preliminary work, some finite-size scaling may be useful in accurately determining any measurable length scale [29].

As discussed earlier, the trap model picture [14,15] may provide a framework for describing the dynamics of our simple granular flow system as well as other supercooled liquids. Trap models are mean field in nature and describe activated dynamics characterized by a probability density of energy barriers and lead to the prediction of trapping time distributions as external parameters such as temperature are varied. To apply these concepts to granular flows, one needs to identify the "traps" and measure the trapping time distributions in order to identify a specific class of trapping models. For the system of inelastic disks studied here, we hope to map the dynamics in the space of the stress tensor to a trap model. This mapping can predict stress autocorrelation functions in steady state and lead to the identification of dynamical phase transitions.

The appearance of frequently and rarely colliding particles with the former associated with the highly stressed regions is reminiscent of the bimodal stress distributions observed in simulations of static, frictional grain packings [30,31], and lend further credence to the idea that the dynamical heterogeneities observed in our simulations are the precursors to force chains in static granular packings. In the dynamical situation, the lifetime of the heterogeneities plays a crucial role and what we have shown is that these heterogeneities become extremely long-lived as the average flow velocity tends to zero.

ACKNOWLEDGMENTS

We thank R. Ravindran, S. Tewari, N. Menon, T. Witten, and P. Sollich for many helpful discussions. A.F. and B.C. acknowledge support from NSF through Grant No. DMR 0207106, and A.F. acknowledges support from the Natural Sciences and Engineering Research Council, Canada.

[1] H. M. Jaeger, S. R. Nagel, and R. P. Behringer, Rev. Mod. Phys. **68**, 1259 (1996).
[2] L. P. Kadanoff, Rev. Mod. Phys. **71**, 435 (1999).
[3] C. H. Liu *et al.*, Science **269**, 513 (1995).
[4] D. M. Mueth, H. M. Jaeger, and S. R. Nagel, Phys. Rev. E **57**, 3164 (1998).
[5] D. Bonamy *et al.*, Phys. Rev. Lett. **89**, 034301 (2002).
[6] O. Pouliquen, Phys. Rev. Lett. **93**, 248001 (2004).
[7] A. Ferguson, B. Fisher, and B. Chakraborty, Europhys. Lett. **66**, 277 (2004).
[8] L. E. Silbert, Phys. Rev. Lett. **94**, 098002 (2005).
[9] E. Weeks *et al.*, Science **287**, 627 (2000).
[10] S. C. Glotzer, V. N. Novikov, and T. B. Schroder, J. Chem. Phys. **112**, 509 (2000).
[11] A. J. Liu and S. R. Nagel, Nature (London) **396**, 21 (1998).
[12] C. S. O'Hern, S. A. Langer, A. J. Liu, and S. R. Nagel, Phys. Rev. Lett. **86**, 111 (2001).
[13] M. E. Cates and P. Sollich, J. Rheol. **48**, 193 (2004).
[14] C. Monthus and J. P. Bouchaud, J. Phys. A **29**, 3847 (1996).
[15] J.-P. Bouchaud, *Slow Relaxations and Nonequilibrium Dynamics in Condensed Matter*, edited by J.-L. Barrat, J. Dalibard, M. Feigelman, and J. Kurchan (Springer, Berlin, 2003).
[16] E. Longhi, N. Easwar, and N. Menon, Phys. Rev. Lett. **89**, 045501 (2002).
[17] C. Denniston and H. Li, Phys. Rev. E **59**, 3289 (1999).
[18] E. Ben-Naim, S. Y. Chen, G. D. Doolen, and S. Redner, Phys. Rev. Lett. **83**, 4069 (1999).
[19] B. Tithi, S. Tewari, A. Ferguson, and B. Chakraborty (unpublished).
[20] S. McNamara and W. R. Young, Phys. Rev. E **50**, R28 (1994).
[21] P. Mills, D. Loggia, and M. Tixier, Europhys. Lett. **45**, 733 (1999).
[22] A. Meheboob and S. Luding, J. Fluid Mech. **476**, 69 (2003).
[23] This change in shape at large impulses is also visible in the impulse distribution $P(\tilde{I}) = \int P(\tilde{I}, \tau) d\tau$.
[24] J. W. Landry (unpublished).
[25] J. Choi, A. Kudrolli, R. R. Rosales, and M. Z. Bazant, Phys. Rev. Lett. **92**, 174301 (2004).
[26] Note that it is possible to have frequently colliding particles with long collision times and rarely colliding particles with short collision times. The frequent-collision criterion is based on an average collision frequency measured over an interval of $\Delta t = 0.02$ and thus reflects that *on average* frequently colliding particles have a shorter average collision time than rarely colliding particles.
[27] W. Kob, *Slow Relaxations and Nonequilibrium Dynamics in Condensed Matter*, edited by J.-L. Barrat, J. Dalibard, M. Feigelman, and J. Kurchan (Springer, Berlin, 2003).
[28] R. Ravindran (unpublished).
[29] L. Berthier, Phys. Rev. Lett. **91**, 055701 (2003).
[30] F. Radjai, D. E. Wolf, M. Jean, and J.-J. Moreau, Phys. Rev. Lett. **80**, 61 (1998).
[31] L. Staron and F. Radjai, Phys. Rev. E **72**, 041308 (2005).